J. Biophoton. **3**, No. 1–2, 25–33 (2010) / **DOI** 10.1002/jbio.200910075

Journal of BIOPHOTONICS

FULL ARTICLE

Monitoring of glucose permeability in monkey skin *in vivo* using Optical Coherence Tomography

Mohamad G. Ghosn[1], *Narendran Sudheendran*[2], *Mark Wendt*[3], *Adrian Glasser*[3], *Valery V. Tuchin*[4,5], *and Kirill V. Larin*[*,1,2,4]

[1] Department of Biomedical Engineering, University of Houston, 4800 Calhoun Rd., N207 Engineering Bldg 1, Houston, Texas 77204-4006, TX USA
[2] Department of Electrical and Computer Engineering, University of Houston, Houston, TX USA
[3] College of Optometry, University of Houston, Houston, TX USA
[4] Institute of Optics and Photonics, Saratov State University, Saratov, Russia
[5] Institute of Precise Mechanics and Control of RAS, Saratov, Russia

Received 31 August 2009, revised 21 September 2009, accepted 22 September 2009
Published online 13 October 2009

Key words: optical coherence tomography, permeability rate, diffusion, skin

Topical trans-dermal delivery of drugs has proven to be a promising route for treatment of many dermatological diseases. The aim of this study is to monitor and quantify the permeability rate of glucose solutions in rhesus monkey skin noninvasively *in vivo* as a primate model for drug diffusion. A time-domain Optical Coherence Tomography (OCT) system was used to image the diffusion of glucose in the skin of anesthetized monkeys for which the permeability rate was calculated. From 5 experiments on 4 different monkeys, the permeability for glucose-20% was found to be $(4.41 \pm 0.28)\ 10^{-6}$ cm/sec. The results suggest that OCT might be utilized for the noninvasive study of molecular diffusion in the multi-layered biological tissues *in vivo*.

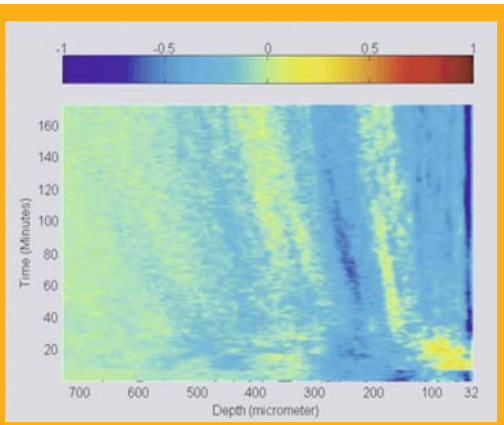

3D representation of glucose diffusion in monkey skin

1. Introduction

Among the many different approaches of drug delivery, such as systemic, intravitreal, oral, buccal, rectal, etc., that are approved by the Food and Drug Administration, the transdermal method offers several advantages such as large accessible areas and being relatively painless [1]. Drug delivery through pills and injections suffers from disadvantages such as metabolic degradation in the intestines and time-variable concentrations in the blood stream. Therefore, topical drug delivery through the skin is a preferable route for many applications and treatments.

* Corresponding author: e-mail: klarin@uh.edu, Phone: (832) 842-8834, Fax: (713) 743-4503

Journal of
BIOPHOTONICS

The skin is the largest organ in the human body and thus plays a number of important roles. For example, skin protects the body against the environment, infections, and excessive fluid loss as well as serves as an important thermoregulatory function. Although a common route for non-invasive drug delivery [2, 3], the skin and most notably the stratum corneum, its outmost layer, is an extremely potent natural barrier; thus, relatively few drugs and macromolecules can penetrate the skin in sufficient quantities to be effective therapeutically. Many skin penetration enhancement studies have been conducted in the past few years [4, 5]. Consequently, techniques have been developed to improve bioavailability and increase the range of drug types used. Some of these methods include the modification of the stratum corneum by hydration [6, 7], the addition of chemical enhancers acting on the structure of the stratum corneum lipids and keratin [8, 9], and the partitioning and solubility effects of the drugs used [10].

Abnormalities in the epithelium and connective tissue of skin may alter the physical and physiological properties of the extracellular matrix, thereby changing the permeability rate of certain drugs or analytes. This change in the permeability rate could be detected and serve as a tool for differentiating between healthy and diseased tissues [11–13]. Furthermore, monitoring and quantifying diffusion through tissues is of great importance for many biological applications, including therapy and diagnostics of several diseases.

Experimental techniques such as spectrofluorometers and Ussing apparatus have been developed to study drug diffusion in tissues [14, 15]. The Ussing chamber allows very accurate measurement of the resistance, current, and voltage, in addition to the impedance and capacitance. By determining the transepithelial electrical potential on each side of the semipermeable membrane, the diffusion rate can be precisely measured. Moreover, fluorescence microscopy [16–18], and microdialysis [19] have also been used in the study of drug diffusion. Microdialysis monitors the chemistry of the extracellular space in the biological tissue. A microdialysis probe mimics a blood capillary into which physiological solution is slowly pumped. As the solution reaches equilibrium with the extracellular tissue fluid, the probe collects a representative sample of the tissue fluid molecules and is then extracted and analyzed in the laboratory. These techniques and more have enhanced the understanding of diffusion of analytes and drugs through tissues; however, these techniques are limited to *in vitro* studies only.

There have also been a few imaging methods capable of assessment the topical drug delivery *in vivo*. For instance, ultrasound has been used in trans-dermal diffusion studies [20], but low resolution and the need for contact procedure limit its applications. Magnetic Resonance Imaging (MRI) has also been proposed as a method for studying transdermal diffusion [21]. MRI could be a very powerful technique in this field; however, there are only a few drugs with paramagnetic properties, and low resolution, long image acquisition and signal processing time requirements of MRI limit its utility.

Optical Coherence Tomography (OCT) is a noninvasive, high-resolution optical imaging technique that has been developed to perform *in vivo* high-resolution, cross-sectional microstructure imaging in biological tissues [22]. Recently, OCT has been introduced to the study of drug and analyte diffusion in aorta, corneal and scleral tissues [11–13, 23–26], as well as in cancerous tissues [27]. Hence, OCT is rapidly establishing itself and being recognized for various applications in medical imaging [28–30]. OCT in its basic configuration uses a Michelson interferometer, illuminated by a low-coherence light source [22]. The light is split by a beam splitter (with various splitting ratio) into a sample and reference path. Light returning from the reference and the sample is recombined at a beam splitter and is recorded by a photodetector in the detection arm of the interferometer. Currently, OCT systems have signal-to-noise ratio (SNR) up to 130 dB. The high SNR is necessary in medical imaging for the detection of the extremely low light intensities typically backscattered from turbid samples such as biological tissue.

Due to many advantages provided by OCT, this study reports the first results (to the best of our knowledge) on the application of OCT for noninvasive monitoring and assessment of passive diffusion of analytes (glucose) *in vivo* in animal skin. The unique capability of OCT for depth-resolved imaging and analysis of tissues' optical properties allowed noninvasive quantification of the glucose permeability rate in monkey skin.

2. Materials and methods

The experiments were conducted using a time-domain OCT (TD-OCT) system (Imalux Corp, Cleveland, OH). Because the tissue being studied undergoes small changes in scattering induced by the molecular movement flux, the high SNR of OCT facilitates clear, precise data for use in the permeability rate calculations. Moreover, monitoring and quantification of relatively slow diffusion processes in skin relaxes the requirement for a fast image acquisition methods. A schematic diagram of the experimental setup is shown in Figure 1. The optical source used in this system is a low-coherent broadband, near-infrared (NIR) light source with wavelength of 1310 $\pm$ 15 nm, output power of 3 mW, and resolution of 25 μm (in air). A single-mode optical fiber and a specially designed miniature endoscopic

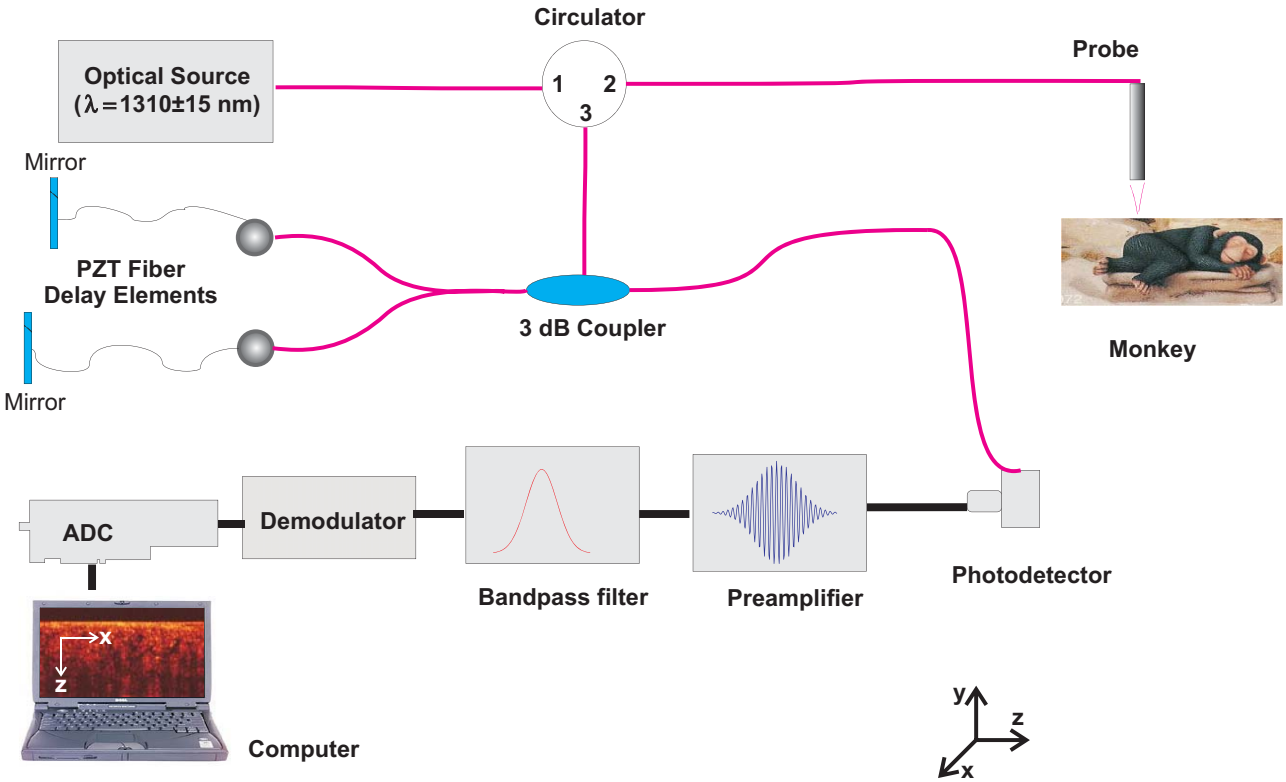

Figure 1 (online color at: www.biophotonics-journal.org) Schematic drawing of the OCT setup used in the experiments.

probe were employed to direct the light of the sample arm of the interferometer into the skin. The endoscopic probe allowed lateral scanning of the sample surface in the lateral direction (X-axis). Light scattered from the sample and light reflected from the reference arm mirror formed an interferogram, which was detected by a photodiode. In-depth scanning was produced electronically by piezo-electric modulation of fiber length in the reference arm of the interferometer. Scanning the incident beam over the sample surface in the lateral direction and in-depth (*Z*-axial) produced two-dimensional OCT images that are 2.2 × 2.4 mm. The full image (450 by 450 pixels) acquisition rate was approximately 3 seconds per image.

All animal experiments were performed in accordance with the Association for Research in Vision and Ophthalmology (ARVO), Statement for the Use of Animals in Ophthalmic and Vision Research, and under an institutionally approved animal protocol. Experiments were performed on rhesus monkeys (*Macaca mulatta,* identified by numbers 34, 54, 96, and 111). The OCT experiments were performed concurrently with other unrelated studies being performed on the monkeys that required anesthesia. Monkeys were initially anesthetized with intramuscular 15 mg/kg ketamine and 0.5 mg/kg acepromazine (Phoenix Pharmaceutical, St. Joseph, MO), and the experiments were performed under intravenous propofol (Propoflo; Abbott Laboratories, North Chicago, IL) anesthesia with an initial bolus of 1.5 mg/kg and a continuous infusion at a rate of 0.5 mg/kg/min. Throughout the experiment, pulse rate, body temperature, and SpO_2 were monitored, and the monkey was wrapped in a 37 °C water-heated pad to maintain body temperature. First, the hair on the right hind leg was shaved. Then, a specially designed plastic probe holder was taped to the shaved skin for about 5 minutes prior to the start of the experiment. 0.2 ml of 20%-concentrated glucose (diluted in distilled water; refractive index – 1.35, pH – 4.6) was topically applied through the hole in the probe holder during the course of imaging and its diffusion in the skin was monitored with OCT as described below.

The permeability rate of glucose in monkey skin was measured by monitoring changes in the OCT signal slope (OCTSS) at a pre-defined in-depth region in the tissue. OCT signal slope is defined as the change in OCT signal value extracted from the OCT images as a function of the distance from the surface of the dermis to a point *x* mm below the dermis. The detailed description of measurement protocol as well as the theoretical description of molecular-induced changes of OCT signal slope are described previously [11, 31–37]. Absorption of glucose in the skin changed the local scattering coefficient and was detected by the OCT system. The penetration of glu-

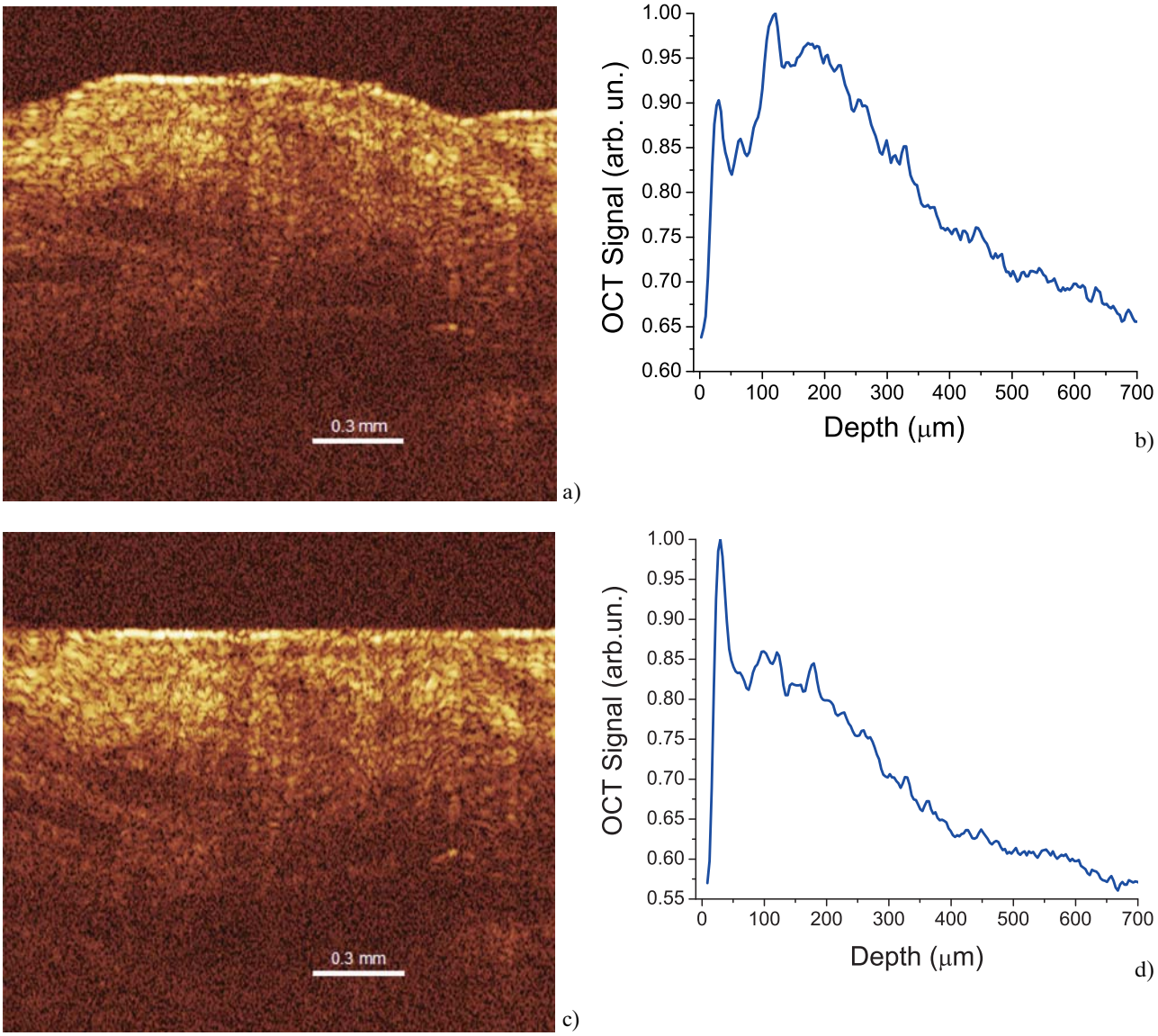

Figure 2 (online color at: www.biophotonics-journal.org) OCT image and corresponding 1D signal recorded from monkey skin *in vivo*.

cose is responsible for the washout of water from the dermis due to the hyperosmotic properties of glucose, thus, the two oppositely directed matter flows (glucose in and water out) lead to the refractive index matching of scatterers and ground (interstitial) material. The increase in the local in-depth concentration of glucose resulted in a progressive decrease in the scattering coefficient and hence in the decrease of the OCT signal slope as a function of time.

First, two-dimensional OCT images (Figure 2a) obtained from the continuous monitoring of the skin optical properties were averaged in the lateral (X-axial) direction into a single logarithmic curve (Figure 2b). In order to clearly distinguish between the different layers of the skin in the images, a program written in Matlab was used to flatten the dermal layer of the tissue to reduce errors caused by local variations in tissue height. The software was written to identify the first value of the first A-scan that is greater than a threshold determined for each image. Then, the rest of the A-scans of each image were aligned according to that first location. Processing the images through this software code aided in differentiating the various layers of the monkey tissue so that diffusion could be clearly discerned in each layer. The results of an image processed through the written Matlab program and its effect on the corresponding 1D logarithmic curve can be seen in Figure 2c and Figure 2d, respectively.

To illustrate the diffusion process as a function of depth and time at the same instance, 1D logarithmic A-scans corresponding to all time points of a typical

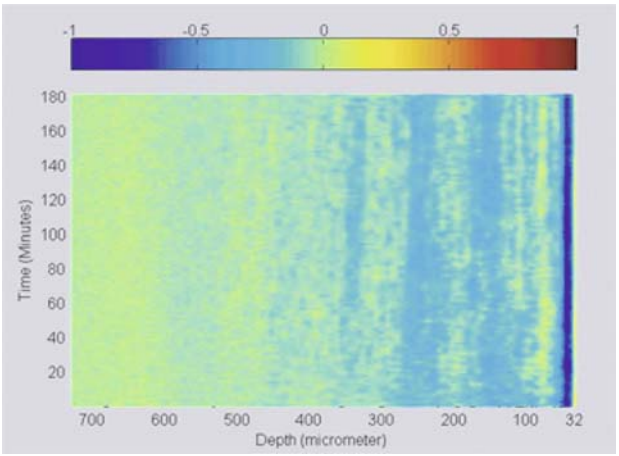

a)

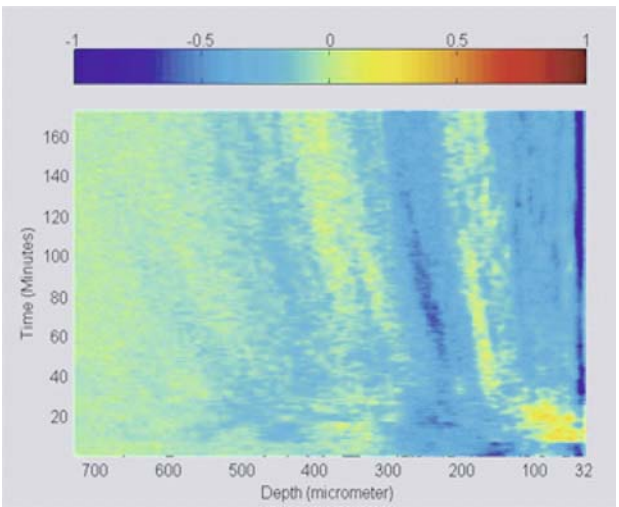

b)

Figure 3 (online color at: www.biophotonics-journal.org) (**a**) 3D representation of a control monkey skin experiment (no glucose added). (**b**) 3D representation of glucose diffusion in monkey skin.

experiment were arranged as a 2D matrix such that the rows of the matrix correspond to the depth and columns to the time. A Matlab program was written to measure and calculate the slope of the signal at all depths of the tissue. To illustrate the diffusion process as shown in Figure 3, the slope data is normalized and set to a color scale. Unlike the OCTSS method which provides the slope at a particular region in the tissue, the 3D diffusion images give a visual representation of slope data over the entire tissue at all depths. As demonstrated by Figure 3(a), the 3D diffusion image of a control experiment does not show any signals of the diffusion whereas the experimental data plotted in Figure 3(b) clearly shows changes in the OCT signal slope (scattering properties) of the tissue while the glucose is diffusing through it.

A region in the tissue, where minimal alteration to the OCT signals occurred with depth (typically – the dermis skin layer), is selected for further time-dependent analysis of its optical properties. The thickness of the chosen section is denoted by z. The diffusion of glucose in the selected area dynamically changed the optical properties of the skin and allowed the calculation of the diffusion time, which was defined as the time taken for the signal to reach a stable minimum time, (t). The permeability rate was then calculated by dividing the thickness of the selected tissue region by the time it took for the glucose to diffuse through $\left(\bar{P} = \frac{z_{\text{region}}}{t_{\text{region}}}\right)$.

3. Results and discussion

Figure 4a shows the typical OCT signal recorded from monkey skin before adding glucose and 60 minutes after adding glucose. The highest peak of the signal represents the beginning of the stratum corneum layer and the rest of the OCT signal is the scattering from the dermal layer of the skin. Due to the addition of glucose, a noticeable change in the slope of the OCT signal is observed, as illustrated in Figure 4b. Figure 5a shows a typical OCT signal slope graph as a function of time for monkey skin *in vivo* during a glucose-20% diffusion experiment. First, the skin was imaged for about 8 minutes to record the OCTSS base line. During this time, a slight increase in the signal slope was observed in all experiments including the control experiment (Figure 5b). After the 8 minute period, 0.2 ml of glucose-20% was topically applied to the OCT scanning area where imaging continued for another 2 hours. The in-depth glucose diffusion process was monitored in a 140 μm thick region 210 μm below the *stratum corneum* layer (dermis region). The increase in the local in-depth glucose concentration resulted in the decrease of the OCTSS during the diffusion process. Flattening of the OCTSS graph indicated the elimination of the refractive index mismatch in the tissue, which was believed to infer that the diffusion of glucose had ceased or reached an equilibrium state. Following this flattening of the OCTSS in the analysis region, an increase in the OCTSS was observed. This could have been the result of a reverse process in the tissue where water began to return in the interior of the tissue. A gradient in the concentration between two sides of a tissue creates a driving force for a fluid to travel from the medium of high concentration to that of a lower one. A smoothed time-signal was obtained by adjacent averaging every 50 points (3 seconds/image = 150 seconds). The permeability rate of glucose in skin was measured in 5 independent experiments from 4 different monkeys,

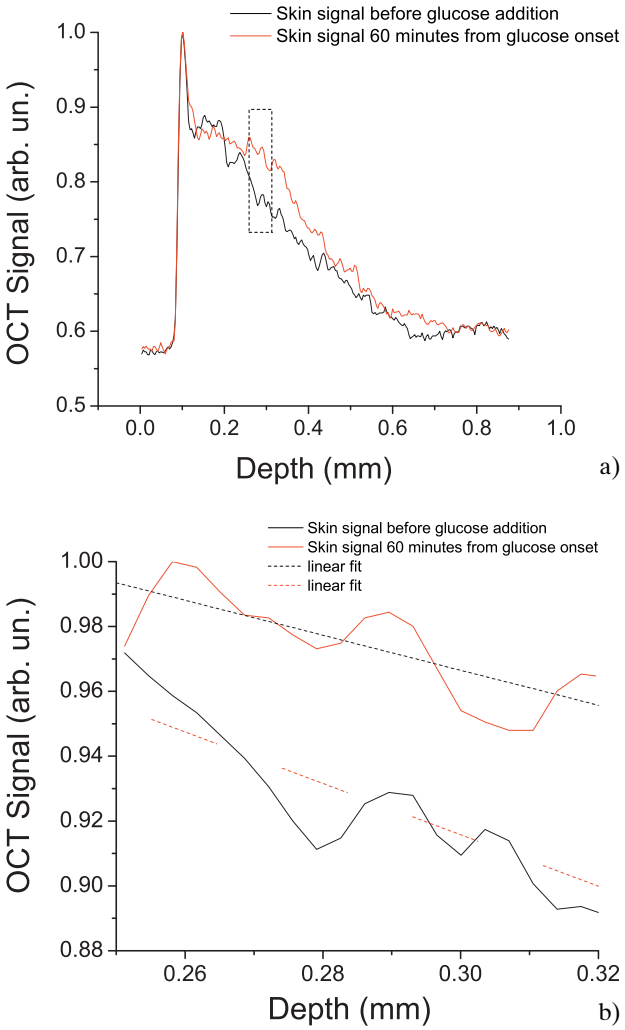

Figure 4 (online color at: www.biophotonics-journal.org) (**a**) Representative OCT signals obtained from monkey skin before adding glucose and 60 minutes after glucose diffusion. (**b**) A part of the OCT signal showing the change in the slope as an effect of the molecular diffusion.

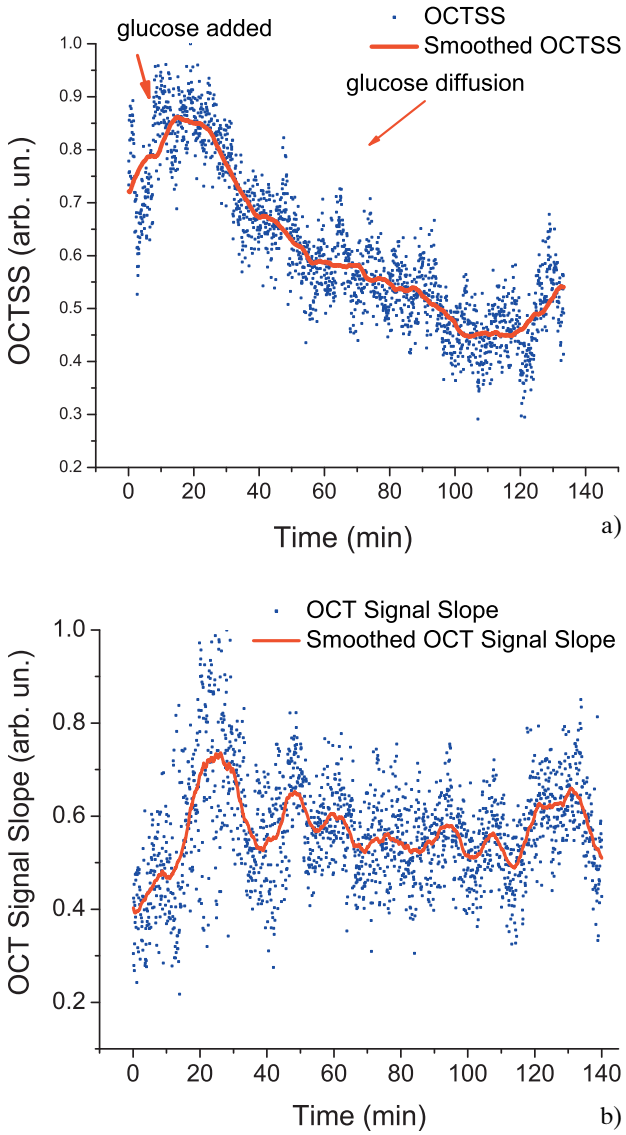

Figure 5 (online color at: www.biophotonics-journal.org) (**a**) OCT Signal slope graph of monkey skin during a glucose 20% diffusion experiment. (**b**) Control OCT Signal slope graph of monkey skin with no glucose added.

which was estimated to be $(4.41 \pm 0.28)\ 10^{-6}$ cm/sec and summarized in Table 1.

Several pathological and disease conditions can change the mechanical properties and ultra-structure of the extracellular matrix (ECM). For example, the increased deposition of ECM proteins and fibroblasts in the stroma surrounding the epithelial cells of the breast is the leading risk factor for breast carcinoma (accounts for 30% of breast cancer) [38]. This and many other diseases might potentially be diagnosed by comparing the permeability rates of several therapeutic or diagnostic agents in normal and abnormal tissues. Therefore, precise assessment of the diffusion processes in normal and abnormal tissues with OCT might provide truly noninvasive way for evaluation of tissue health [11, 13].

Table 1 Permeability rate of glucose 20% in separate monkey experiments.

Monkey number	Permeability rate (cm/sec)
54	4.68×10^{-6}
96	4.17×10^{-6}
111	3.54×10^{-6}
34	4.96×10^{-6}
54	4.70×10^{-6}
Average ± Standard deviation	$(4.41 \pm 0.28) \times 10^{-6}$

For the permeability rate calculations, the refractive index for the skin was assumed to be uniform and equal to 1.4. This assumption is not entirely correct for two main reasons: 1) molecular diffusion into the monitored region will dynamically change the local value for the refractive index and 2) the local value for the refractive index might be not uniformly distributed across the selected region. A comparison between the control and other experiments indicated that the diffusion of glucose is what changed the refractive index during the course of the experiment and therefore determined the size of the region selected for calculations. Glucose induces a change in the refractive index of 2.5×10^{-5} per mM [39]. Therefore, the maximal changes of the local refractive index for glucose-20% in the 140 micron region shown in Figure 5a is 2.8×10^{-2} which would result in a dimensional change in the tissue being imaged of 3.9 μm – the absolute value of the error in thickness determination. This error would lead to the error of the measured permeability rate by 2.2%, which is within the standard deviation of the experimental data presented in this paper. Thus, the difference is small and was not considered in our calculations of the permeability rates presented. In addition, the skin is a turbid non-uniform tissue with some variation in the refractive index through its layers. Nevertheless, a correction that accounts for the change of local refractive index and its influence on the accuracy of the permeability rates calculations will be done in our future studies.

The OCT signal slope measured in the dermis region might have been sensitive to changes induced by glucose in the stratum corneum layers [40]; thus, the slope could not only be carrying information about the permeability in the dermis region but also from the above layers such as the epidermis as well. However in a study by Schmitt et al. [41] using scattering media with two layers of different attenuation coefficients found that the scattering coefficient of the second layer was not dependent on the properties of the first layer. Similarly, since skin is composed of the outer stratum corneum layer and the dermis region below, it can be presumed that the measured slope in dermis region is not affected by the changes in optical properties in the stratum corneum layer. Hence, any changes in measured slope of dermis region are because of changes in scattering properties of the region brought about by diffusion of glucose into the region.

In all trials conducted, an increase in the signal slope was observed at the very beginning of the experiment. We speculate that the tissue's physiological response to the pressure introduced to the monkey skin by adding the probe-holder might have played a role in this change. Compressing soft tissues while applying some local pressure would instigate water displacement causing a reduction in the overall tissue thickness. This phenomenon was shown to initiate an increase in the scattering in the tissue during *in vitro* experiments [42]. These changes could be unidirectional (both increase) or have an opposite direction (scattering coefficient decrease and absorption increase) in dependence of compression mode (uniformly distributed or point-wise). This could have also resulted from preventing surface evaporation and therefore changing the moisture gradient, the density gradient, and the refractive index gradient in the skin. This issue will be investigated in more detail in future experiments to show the effect's prevalence in *in vivo* experiments as well.

4. Conclusion

The OCT noninvasive and nondestructive functional imaging technique shows promise as a tool for the study of drug and analyte diffusion. In this study, the permeability rate of glucose through rhesus monkey skin *in vivo* was quantified. By measuring the glucose-induced changes in refractive index within the tissue, the permeability rate was calculated. OCT's noninvasive and nondestructive capabilities allow for high accuracy and little variance among the different monkeys. Some image processing techniques were utilized on the acquired images to reduce tissue curvature and eliminate the error caused by it. The mean permeability rate of glucose-20% was calculated to be $(4.41 \pm 0.28) \times 10^{-6}$ cm/sec from five independent experiments. The small standard deviation of the permeability rate suggests high accuracy of the OCT-based method for assessment of molecular diffusion processes in skin and relatively low variability of skin structure from monkey to monkey. These results may serve as a useful permeability model for future studies and considerations regarding topical dermatological drugs.

Acknowledgements This study was funded in part by grants from NIH R01 HL095586, Office of Naval Research N000140710943, (KVL), NEI grant #1 RO1 EY014651 (AG), CRDF RUB1–2932-SR-08, and Federal Agency of Education of RF 2.1.1/4989, 2.2.1.1/2950, and 1.4.09, President of the RF 208.2008.2, FP7-ICT-2007–2 PHOTONICS4LIFE (No. 224014) (VVT). The authors would like to thank Mr. Michael Leba, and Ms. Astha Vijayanada for their contributions to this manuscript.

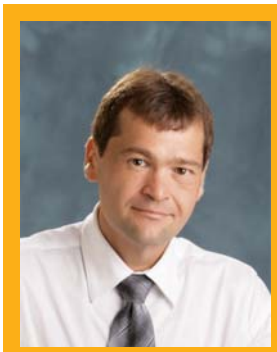

Kirill V. Larin, Ph.D. is Assistant Professor of Biomedical Engineering at the University of Houston, TX. His research interests focus on development and application of OCT for noninvasive and nondestructive imaging and diagnostics of tissues and cells. Dr. Larin has authored more than 40 peer-reviewed journal publications and chapters in two textbooks on Biomedical Optics. He is recipient of Boris Yeltsin Presidential Award, Wallace Coulter Young Investigator Translation Award, Office of Naval Research Young Investigator Award, and Outstanding Young Investigator Award from the Houston Society for Engineers in Medicine and Biology.

Mohamad G. Ghosn, Ph.D. is a post-doctorate researcher at the Biomedical Optics Laboratory at the University of Houston. Among his research interests is the assessment of molecular diffusion of various drugs and analytes across biological tissues using Optical Coherence Tomography. He has had the opportunity to publish his work in 11 papers and he also enjoys teaching for which he was awarded the Outstanding Teacher Assistant Award for the year 2008 from the Cullen College of Engineering. His career goal is to become a professor in Biomedical Engineering.

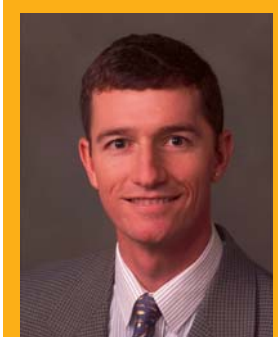

Adrian Glasser, Ph.D. is a Professor of Optometry and Vision Sciences and Biomedical Engineering and the Benedict-Pits Professor at the University of Houston. Before he joined the College of Optometry as an Assistant Professor in 1998, he completed a B.S. degree in biology and an M.S. degree in neurobiology at the State University of New York at Albany in 1990. In 1994, he obtained a Ph.D. degree in physiology from Cornell University Ithaca, N.Y. Following that, Dr. Glasser completed postdoctoral research fellowships at the University of Waterloo School of Optometry and in the Department of Ophthalmology and Visual Sciences at the University of Wisconsin-Madison. Dr. Glasser is actively pursuing federally funded and industry funded research on the physiology and optics of accommodation and presbyopia.

Valery V. Tuchin holds the Optics and Biophotonics Chair and is a Director of Research-Educational Institute of Optics and Biophotonics at Saratov State University. He has authored more than 300 peer-reviewed papers and books, including his latest, Tissue Optics (PM166, SPIE Press, 2007) and Handbook of Optical Sensing of Glucose in Biological Fluids and Tissues (CRC Press, 2009). He has been awarded RF Honored Science Worker and SPIE Fellow; he is a Vice-President of Russian Photobiology Society. In 2007 he has been awarded the SPIE Educator Award.

Mark Wendt, M.S. is a Laboratory Manager in the Optometry School at the University of Houston, TX. He has worked primarily in the field of Vision Sciences where he has been an author on seven papers. His recent research interests have focused on image processing and image analysis.

Narendran Sudheendran is a M.S. student in the Electrical and Computer Engineering at the University of Houston, TX. His focus is quantification of blood flow in tissues using Speckle and Doppler Optical Coherence Tomography

References

[1] W. T. Zempsky, Pediatrics **101**, 730-1 (1998).
[2] G. Cevc, Clin. Pharmacokinet. **42**, 461–474 (2003).
[3] J. Y. Fang and Y. L. Leu, Curr. Drug Discov. Technol. **3**, 211–224 (2006).

[4] H. Benson, Current Drug Delivery **2**, 23–33 (2005).
[5] K. Walters and J. Hadgraft, Pharmaceutical Skin Penetration Enhancement New York, New York: Marcel Dekker, Inc., 1993.
[6] R. J. Scheuplein and I. H. Blank, Physiol Rev **51**, 702–747 (1971).
[7] R. J. Scheuplein and I. H. Blank, J. Invest. Dermatol. **60**, 286–296 (1973).
[8] M. A. Yamane, A. C. Williams, and B. W. Barry, J. Pharm. Pharmacol. **47**, 978–989 (1995).
[9] K. A. Walters, M. Walker, and O. Olejnik, J. Pharm. Pharmacol. **40**, 525–529 (1988).
[10] Shishu and N. Aggarwal, Int. J. Pharm. **326**, 20–24 (2006).
[11] M. G. Ghosn, E. F. Carbajal, N. Befrui, A. Tellez, J. F. Granada, and K. V. Larin, J. Biomed. Opt. **13**, 010505(3) (2008).
[12] K. V. Larin and V. V. Tuchin, Quantum Electronics **38**, 551–556 (2008).
[13] M. Ghosn, M. Leba, A. Vijayananda, P. Rezaee, J. D. Morrisett, and K. V. Larin, J. Biophoton., vol. doi: 10.1002/jbio.200810071 2009.
[14] K. Okabe, H. Kimura, J. Okabe, A. Kato, H. Shimizu, T. Ueda, S. Shimada, and Y. Ogura, Invest. Ophthalmol. Vis. Sci. **46**, 703–708 (2005).
[15] J. W. Kim, J. D. Lindsey, N. Wang, and R. N. Weinreb, Invest. Ophthalmol. Vis. Sci. **42**, 1514–1521 (2001).
[16] J. D. Lindsey and R. N. Weinreb, Invest. Ophthalmol. Vis. Sci. **43**, 2201–2205 (2002).
[17] J. Ambati, C. S. Canakis, J. W. Miller, E. S. Gragoudas, A. Edwards, D. J. Weissgold, I. Kim, F. C. Delori, and A. P. Adamis, Invest. Ophthalmol. Vis. Sci. **41**, 1181–1185 (2000).
[18] T. W. Kim, J. D. Lindsey, M. Aihara, T. L. Anthony, and R. N. Weinreb, Invest. Ophthalmol. Vis. Sci. **43**, 1809–1816 (2002).
[19] C. J. Morgan, A. G. Renwick, and P. S. Friedmann, Br J. Dermatol. **148**, 434–443 (2003).
[20] D. Bommannan, H. Okuyama, P. Stauffer, and R. H. Guy, Pharm. Res. **9**, 559–564 (1992).
[21] R. A. Carano, A. L. Ross, J. Ross, S. P. Williams, H. Koeppen, R. H. Schwall, and N. Van Bruggen, Magn. Reson. Med. **51**, 542–551 (2004).
[22] D. Huang, E. A. Swanson, C. P. Lin, J. S. Schuman, W. G. Stinson, W. Chang, M. R. Hee, T. Flotte, K. Gregory, and C. A. Puliafito, et al., Science **254**, 1178–1181 (1991).
[23] M. G. Ghosn, V. V. Tuchin, and K. V. Larin, Opt. Lett. **31**, 2314–2316 (2006).
[24] K. V. Larin and M. G. Ghosn, Quantum Elect. **36**, 1083–1088 (2006).
[25] K. V. Larin, M. G. Ghosn, S. N. Ivers, A. Tellez, and J. F. Granada, Laser Phys. Lett. **4**, 312–317 (2007).
[26] M. G. Ghosn, V. V. Tuchin, and K. V. Larin, Invest. Ophthalmol. Vis. Sci. **48**, 2726–2733 (2007).
[27] H. Xiong, Z. Guo, C. Zeng, L. Wang, Y. He, and S. Liu, J. Biomed. Opt. **14**, 024029-5 (2009).
[28] A. M. Zysk, F. T. Nguyen, A. L. Oldenburg, D. L. Marks, and S. A. Boppart, J. Biomed. Opt. **12**, 051403 (2007).
[29] D. Stifter, Appl. Phys. B-Lasers Opt. **88**, 337–357 (2007).
[30] P. H. Tomlins and R. K. Wang, J. Phys. D Appl. Phys. **38**, 2519–2535 (2005).
[31] I. V. Larina, E. F. Carbajal, V. V. Tuchin, M. E. Dickinson, and K. V. Larin, Laser Phys. Lett. **5**, 476–480 (2008).
[32] M. G. Ghosn, E. F. Carbajal, N. Befrui, V. V. Tuchin, and K. V. Larin, J. Biomed. Opt. **13**, 021110-1-021110-6 (2008).
[33] M. Ghosn, V. V. Tuchin, and K. V. Larin, Invest. Ophth. Vis. Sci. **48**, 2726–2733 (2007).
[34] M. Ghosn, V. V. Tuchin, and K. V. Larin, Opt. Lett. **31**, 2314–2316 (2006).
[35] K. V. Larin, M. Motamedi, T. V. Ashitkov, and R. O. Esenaliev, Phys. Med. Biol. **48**, 1371–1390 (2003).
[36] K. V. Larin, M. S. Eledrisi, M. Motamedi, and R. O. Esenaliev, Diabetes Care **25**, 2263–2267 (2002).
[37] R. O. Esenaliev, K. V. Larin, I. V. Larina, and M. Motamedi, Opt. Lett. **26**, 992–994 (2001).
[38] N. F. Boyd, G. A. Lockwood, J. W. Byng, D. L. Tritchler, and M. J. Yaffe, Cancer Epidemiol. Biomarkers Prev. **7**, 1133–44 (1998).
[39] R. C. Weast, Handbook of Chemistry and Physics vol. 11. Cleveland, Ohio: The Chemical Rubber Co., 1972.
[40] M. J. Yadlowsky, J. M. Schmitt, and R. F. Bonner, Appl. Opt. **34**, 5699–5707 (1995).
[41] J. M. Schmitt, A. Knuttel, and R. F. Bonner, Appl. Opt. **32**, 6032–6042 (1993).
[42] V. V. Tuchin, Optical Clearing of Tissues and Blood Bellingham, WA: SPIE Press (2006).